Available online at www.sciencedirect.com

ScienceDirect

Virology 365 (2007) 336–345

VIROLOGY

www.elsevier.com/locate/yviro

Impact of *in vitro* assembly defects on *in vivo* function of the phage P22 portal☆

Ying Sun, Stacy A. Overman, George J. Thomas, Jr.*

Division of Cell Biology and Biophysics, School of Biological Sciences, University of Missouri–Kansas City, 5100 Rockhill Road, Kansas City, MO 64110, USA

Received 2 January 2007; accepted 12 February 2007
Available online 9 May 2007

Abstract

The podovirus P22, which infects *O*-antigen strains of *Salmonella*, incorporates a dsDNA translocating channel (portal dodecamer) at a unique vertex of the icosahedral capsid. The portal subunit (gp1, 82.7 kDa) exhibits multiple S–H···X hydrogen bonding states for cysteines 153, 173, 283 and 516 and these interactions are strongly perturbed by portal ring formation. Here, we analyze *in vivo* activities of wild type (wt) and Cys→Ser mutant portals, demonstrate that *in vivo* activity is correlated with *in vitro* assembly kinetics, and suggest mechanistic bases for the observed assembly defects. The C283S portal protein, which assembles into rings at about half the rate of wt, exhibits significantly diminished infectivity (~50% of wt) and manifests its defect prior to DNA packaging, most likely at the stage of procapsid assembly. Conversely, the C516S mutant, which assembles at twice the rate of wt, is more severely deficient *in vivo* (~20% of wt) and manifests its defect subsequent to capsid maturation and DNA packaging. Both C153S and C173S portals function at levels close to wt. The results suggest that C283S and C516S mutations may be exploited for improved characterization of the folding and assembly pathway of P22 portal protein.

Keywords: Bacteriophage; P22; Portal; Protein; Structure; Assembly; Function; Raman spectroscopy

Introduction

P22 is a member of the *Podoviridae* family of short-tailed bacteriophages that infect strains of *Salmonella typhimurium* presenting a repetitive *O*-antigen structure along the lipopolysaccharide surface. The mature phage consists of a 43.4-kbp dsDNA genome packaged within an icosahedral capsid comprising 420 copies of a 46.8-kDa coat protein (gp5), 12 copies of an 82.7-kDa portal protein (gp1), 3 to 12 copies of each of three ejection proteins (gp7, 23.4 kDa; gp16, 6.4 kDa; gp20, 50.1 kDa) and three portal completion proteins (gp4, 18.0 kDa; gp10, 52.5 kDa; gp26, 24.7 kDa), and 6 tailspikes, each formed from 3 copies of a 71.9-kDa subunit (gp9) (King et al., 1973; Botstein et al., 1973; Prevelige and King, 1993; Fane and Prevelige, 2003; Casjens and Weigele, 2005). The portal dodecamer, which is located at a unique fivefold vertex of the $T=7$ icosahedral capsid, has been considered pivotal to many steps in virion assembly, including construction of the capsid precursor shell (procapsid) (Bazinet et al., 1988; Bazinet and King, 1988; Greene and King, 1996; Moore and Prevelige, 2002a; Weigele et al., 2005), reorganization of the procapsid lattice during maturation (Moore and Prevelige, 2002a, 2002b), packaging of the viral genome (Casjens et al., 1992; Moore and Prevelige, 2002b), closure of the portal channel and attachment of the tail apparatus (Strauss and King, 1984; Tang et al., 2005).

Molecular mechanisms governing the morphogenesis of bacteriophage P22 provide useful prototypes for understanding assembly pathways of many eukaryotic dsDNA viruses, including the *Herpesviridae* (Newcomb et al., 2003; Trus et

Abbreviations: dsDNA, double-stranded deoxyribonucleic acid; EDTA, ethylenediaminetetraacetic acid; EM, electron microscopy; gp, gene product; HPSEC, high performance size exclusion chromatography; IPTG, isopropyl-β-D-thiogalactopyranoside; kbp, kilo base pair; kDa, kilo Dalton; MDa, mega Dalton; SDS–PAGE, sodium dodecyl sulfate polyacrylamide gel electrophoresis; SE, sedimentation equilibrium; SEC, size exclusion chromatography; SH, sulfhydryl; $t_{1/2}$, half-life; Tris, tris(hydroxymethyl)aminoethane; UV, ultraviolet; wt, wild type.

☆ Part LXXXVII in the series Structural Studies of Viruses by Raman spectroscopy.

* Corresponding author. Fax: +1 816 235 1503.
E-mail address: thomasgj@umkc.edu (G.J. Thomas).

0042-6822/$ - see front matter © 2007 Elsevier Inc. All rights reserved.
doi:10.1016/j.virol.2007.02.040

al., 2004). An overview of the P22 assembly pathway is represented schematically in Fig. 1. Roles of scaffolding and capsid proteins in this pathway have been extensively investigated; however, the role of the portal remains less well understood.

The portal subunit contains 725 amino acids, including four cysteines that are widely distributed through the sequence (Cys 153, Cys 173, Cys 283, Cys 516) (Eppler et al., 1991). Although no high-resolution structure is currently available for either the isolated gp1 subunit or its oligomeric ring, the secondary and tertiary structures of gp1 monomers and rings were characterized previously by methods of Raman spectroscopy (Rodriguez-Casado et al., 2001). In addition, the S–H···X hydrogen bonding states of the four cysteines were identified as a function of *in vitro* ring assembly (Rodriguez-Casado and Thomas, 2003). The P22 portal assembly has been characterized as a dodecamer based on both negative-stain electron microscopy (EM) of rings produced *in vitro* (Bazinet et al., 1988) and cryo-EM reconstructions of tails *in situ* (Lander et al., 2006) or extracted from mature virions (Tang et al., 2005). A preliminary crystallographic analysis of the portal dodecamer has also been reported (Cingolani et al., 2002). Very recently, it has been shown that both undecameric and dodecameric ring states of the P22 portal protein are stable *in vitro* (Poliakov et al., 2007).

Our previous Raman studies have shown that local environments of many gp1 side chains, including cysteines, tyrosines and tryptophans, are altered dramatically by ring formation even though very little overall change occurs in the ordered secondary structure of the subunit (~57% α-helix, ~26% β-strand) (Rodriguez-Casado et al., 2001; Rodriguez-Casado and Thomas, 2003). The data suggest domain movements involving much of the protein, including a portion of the sequence (residues 240–350) that exhibits secondary structure homology with residues 125–225 of the bacteriophage φ29 portal (connector) (Simpson et al., 2000; Rodriguez-Casado et al., 2001). In the φ29 connector crystal structure the latter sequence contributes to the surfaces of the DNA-translocating channel and subunit interface. Although only one cysteine of the P22 portal subunit (Cys 283) occurs within the putative homology domain, side-chain interactions of all four cysteines are demonstrably sensitive to the state of portal assembly. Specifically, all cysteines exhibit stronger S–H···X hydrogen bonding interactions in the monomer than in the dodecamer (Rodriguez-Casado and Thomas, 2003). A preliminary analysis of the *in vitro* assembly defects of the Cys→Ser mutants has been reported (Rodriguez-Casado and Thomas, 2003).

Here, we present a more detailed quantitative assessment of portal assembly kinetics using size exclusion chromatography (SEC) for the wt and Cys→Ser mutant proteins, report the relative infectivities of virions incorporating wt and mutant portals, and demonstrate that the *in vitro* portal assembly defects correlate with *in vivo* phage activity. We also present the results of sedimentation equilibrium measurements on wt and mutant portals, which extend previously reported measurements on the wt monomer (Moore and Prevelige, 2001). The correlations established here may provide benchmarks for future assessment of portal protein interactions with other phage structural proteins that participate in late stages of the virion assembly pathway (Fig. 1).

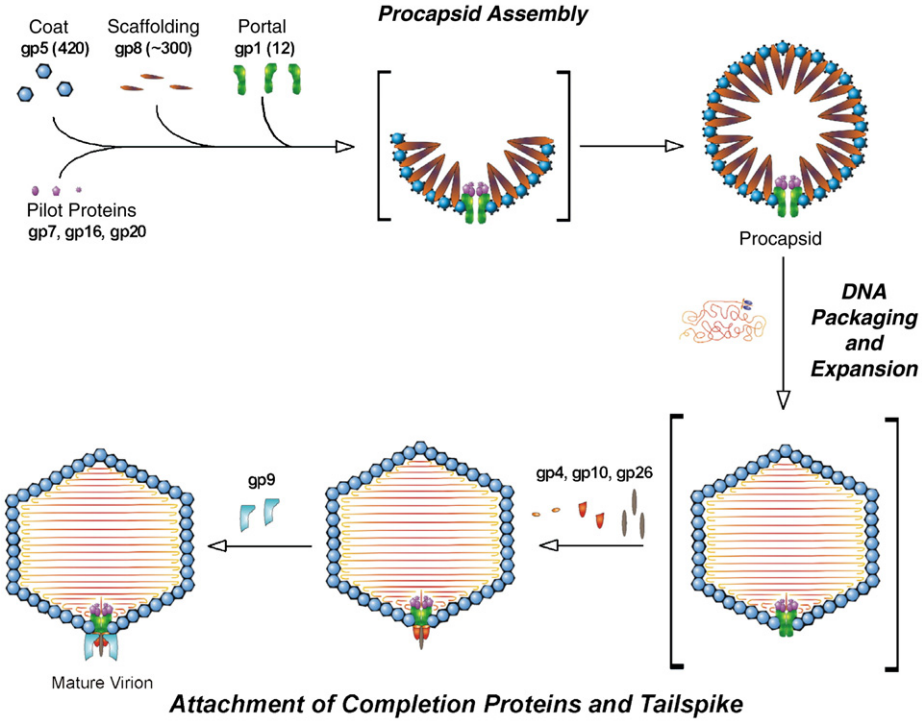

Fig. 1. P22 assembly pathway showing procapsid formation involving coat, scaffolding and portal subunits (top, left-to-right). Scaffolding is eliminated from the procapsid interior concurrent with DNA packaging and shell expansion (right, top-to-bottom). Subsequent steps involve attachment of portal completion proteins and tailspikes to the mature capsid (bottom, right-to-left) (King et al., 1976; Fane and Prevelige, 2003).

Results

Oligomerization rates of portal variants

The well-resolved HPSEC elution peaks of portal protein monomer and dodecamer (Fig. 2A, insert) and the readily monitored time dependencies of their HPSEC elution profiles (Fig. 2A and corresponding data on C153S and C173S not shown) provide a basis for accurate evaluation of *in vitro* portal assembly rates (Fig. 2B). The data shown in Fig. 2, which were collected from 50 μg/μL protein solutions in buffer A at 4 °C, are consistent with the kinetics data reported previously for wt portal assembly within the temperature interval 15–30 °C (Moore and Prevelige, 2001). We employed 4 °C here to decelerate the dodecamerization reaction and enable more precise measurement of the gp1 assembly rate. Importantly, the present results refine the previously proposed rough estimates of mutant assembly kinetics in low salt buffer (Rodriguez-Casado and Thomas, 2003), where competing disassembly events were not explicitly taken into account. The precision of the results shown in Fig. 2B permits a clear-cut distinction between mutant portals (C153S and C173S) that exhibit assembly rates very similar to wt and those (C283S and C516S) that exhibit highly disparate assembly rates. The times required for 50% assembly of each portal variant at the *in vitro* conditions specified in the Fig. 2 legend are as follows: $t_{1/2}^{wt}=42$ h, $t_{1/2}^{C153S}=44$ h, $t_{1/2}^{C173S}=36$ h, $t_{1/2}^{C283S}=90$ h, $t_{1/2}^{C516S}=20$ h. Thus, the C283S mutation significantly impedes *in vitro* assembly, presumably by hyperstabilizing the monomer state, while the C516S mutation has the reverse effect. All variants achieve >95% assembly, as verified by SEC after incubation of the monomer at 22 °C for 24 h.

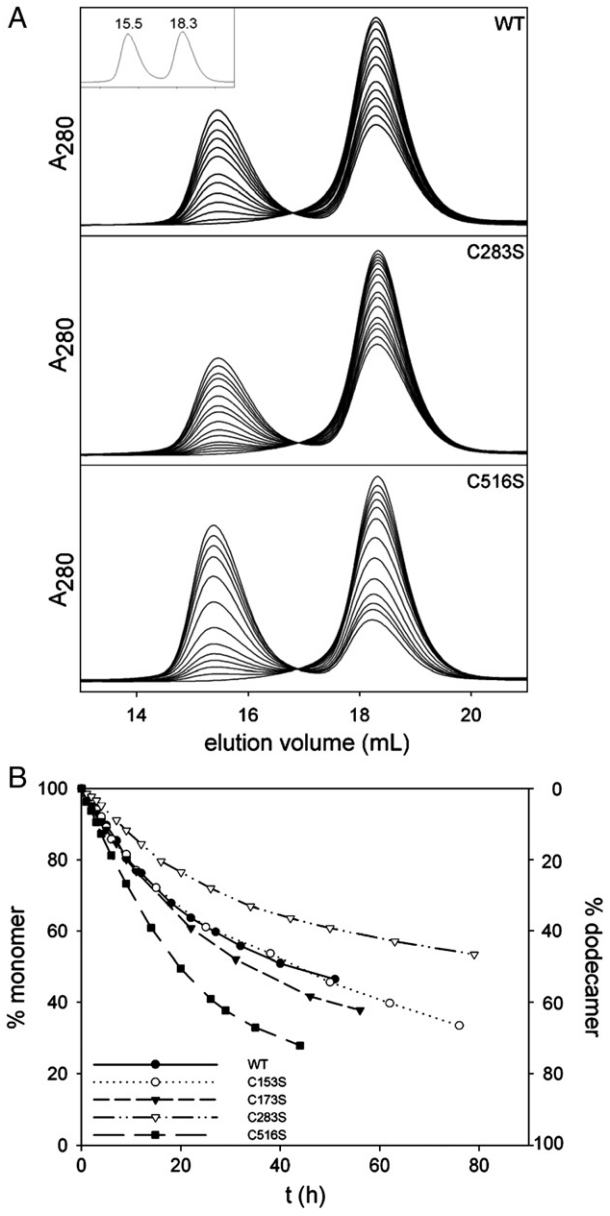

Fig. 2. (A) HPSEC profiles of the monomer→dodecamer oligomerizations of wt (top), C283S (middle) and C516S (bottom) portals. In each case, the monomer and dodecamer elution volumes are at 18.3 and 15.5 mL, respectively. For wt, the chromatograms were recorded at 0, 1, 3, 5, 7, 9, 12, 18, 22, 27, 32, 40 and 51 h after incubation of a 50 μg/μL solution at 4 °C. (The inset at upper left shows the 40-h chromatogram trace, in which the relative peak areas correspond to 52% monomer and 48% dodecamer.) For C283S, data are shown for 0, 1, 2, 3, 4, 7, 9, 12, 16, 20, 26, 32, 42, 50, 63 and 79 h. For C516S, data are shown for 0, 1, 2, 3, 4, 6, 9, 14, 20, 26, 29, 35 and 44 h. (B) Rates of oligomerization of wt and Cys→Ser mutant portals, as labeled.

Table 1
Relative biological activities of wt and Cys→Ser mutant portal rings[a]

Portal	28 °C	37 °C	42 °C	45 °C
wt	100	100	100	60
C153S	70±4	71±4	69±4	43±4
C173S	72±4	70±4	71±4	42±4
C283S	48±4	47±4	49±4	30±2
C516S	19±2	18±2	5±1	2±1

[a] Entries are the percentages of wt activity (arbitrarily 100% for the recombinant His_6-tagged protein at 37 °C), as measured by the number of PFUs in complementation assays at the indicated growth temperatures. Protocols are described in the text. As shown previously (Moore and Prevelige, 2001), the recombinant His_6-tagged protein exhibits 50% of the activity of the native wild type sequence.

The isosbestic points evident in the data of Fig. 2A (and in additional data on C153S and C173S not shown) demonstrate that *in vitro* assembly of each portal variant occurs without significant accumulation of intermediates along the assembly pathway. This finding is of relevance to the Raman experiments described below, for which identical protein concentrations of 50 μg/μL were employed.

Biological activities of portal variants

Assessment of the relative biological activities of wt and Cys→Ser mutant portals expressed *in vivo* from inducible plasmids indicates that only the mutants C283S and C516S exhibit activities less than 50% that of wt (Table 1). Biological activities were monitored using complementation assays in which *S. typhimurium* cells containing the gp1 expressing plasmid were infected with *1⁻13⁻ amber* mutant phage and simultaneously induced to express gp1. The cultures were grown at 37 °C, which is optimal for *S. typhimurium* cells and P22 phage. Activities were quantified in terms of the number of

infectious particles produced, as assessed from titers of the cell lysates. The results, as listed in Table 1, indicate modest activity defects (~30%) for C153S and C173S, compared with the more serious defects for C283S (53%) and C516S (82%). We conclude that a Ser substitution for Cys 283 or Cys 516 seriously impairs portal function. The corresponding *in vitro* studies noted above imply that the *in vivo* defects occur at the level of monomer→dodecamer assembly kinetics.

Additional complementation assays revealed that all portal protein present in each cell lysate was expressed from the inducible plasmid and not from the P22 genome. For such controls, which produced no phage, the host was infected with *1⁻13⁻* phage but not induced to express gp1. On the basis of these findings, we conclude that in each infection (wt, C153S, C173S, C283S, C516S) all of the gp1 available for virion assembly was induced from the gp1-expressing plasmid. Therefore, the biological activities determined in the complementation assays of Table 1 reliably quantify *in vivo* activities of the portal variants.

Molecular basis of mutant portal defects

To gain further insight into the likely sources of the infectivity defects exhibited by P22 particles incorporating the different portal variants, we examined soluble components of the respective cell lysates using sucrose gradient analysis and SDS–PAGE. Previous analyses of lysates of P22-infected cells using similar methods (Fuller and King, 1980; Moore and Prevelige, 2002b) provide a basis for distinguishing mature virions (DNA-filled capsids, bottom of gradient) from procapsids or procapsid-like particles (devoid of DNA, middle of gradient). Fig. 3 compares the results obtained for wt, C173S, C283S and C516S. (Not shown are the results obtained for C153S, which are indistinguishable from wt.) Lanes 7, 8 and 9 of each gel of Fig. 3 show electrophoresis patterns of middle gradient fractions 7, 8 and 9, respectively, which contain the bulk of procapsids and procapsid-like species. Lanes 7, 8 and 9 of the wt gel (Fig. 3, top) clearly reveal that gp1 (portal), gp5 (coat) and gp8 (scaffold) are the most abundant protein components, as expected for native P22 procapsids. These particles are competent to package DNA and lead to the bottom gradient fraction (lane 12) that is dominated by gp1 and gp5. (See also Fig. 3 legend.) Similar results apply to C173S (Fig. 3, second from top), C516S (Fig. 3, bottom) and C153S (not shown). On the other hand, the corresponding lanes of the C283S gel (Fig. 3, second from bottom) are relatively deficient in the portal protein gp1, despite abundant populations of gp5 and gp8, thus signaling the presence of a substantial proportion of procapsid-like particles lacking portal. It is clear from lane 12, however, that a significant population of native C283S procapsids was also formed and underwent DNA packaging. We conclude that the Cys 283→Ser mutation introduces an assembly defect *in vivo* at the level of portal incorporation into the procapsid, and that this defect diminishes but does not totally preclude the formation of a subpopulation of native procapsids competent to package DNA. Because C283S portal protein dodecamerization *in vitro* is appreciably retarded vis-à-vis wt (Fig. 2), it seems likely that the C283S mutation introduces a kinetic barrier to portal ring formation *in vivo*.

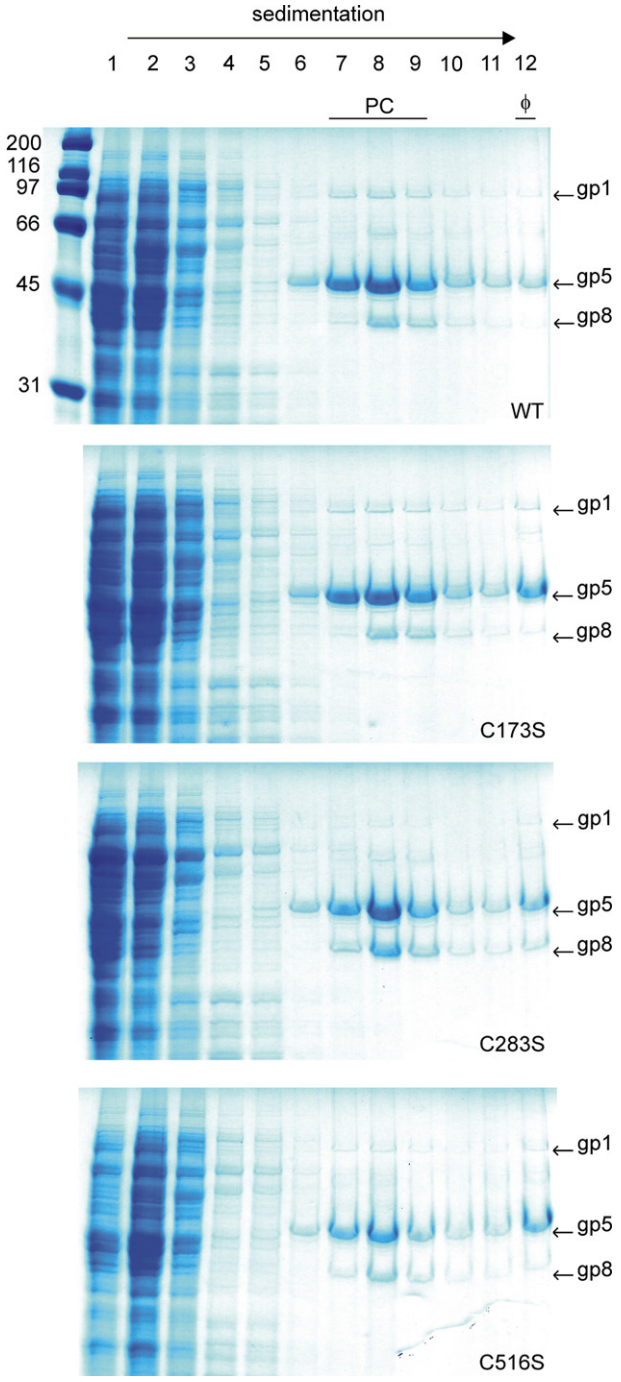

Fig. 3. SDS–PAGE detection of portal protein in sucrose gradient fractions of the cell lysates obtained from complementation assays for wt, C173S, C283S and C516S portal variants. (Results for the C153S variant, not shown, are similar to those shown for wt, C173S and C516S variants.) In the top gel, which corresponds to wt, molecular weight standards are shown in the lane to the left of lane 1; the lanes labeled 1–12 correspond to fractions containing species of increasing sedimentation coefficient; the fractions containing DNA-free procapsids and DNA-filled capsids are labeled PC and φ, respectively; and bands of the portal (gp1), coat (gp5) and scaffolding (gp8) proteins are indicated by the labels at the right (Fuller and King, 1980; Moore and Prevelige, 2001). The same gel assignments apply to the mutants.

Table 2
Thermostabilities of capsid-incorporated wt and Cys → Ser mutant portal rings[a]

Portal	45 °C, 5 h	45 °C, 15 h	55 °C, 5 h	55 °C, 15 h
wt	92±10	97±4	104±6	97±8
C153S	99±9	93±9	107±5	97±13
C173S	92±4	93±4	104±9	91±10
C283S	110±8	93±9	101±12	97±7
C516S	95±5	88±9	80±5	29±4

[a] Entries are the percentages of wt activity (arbitrarily 100% for phage incubated 15 h at 4 °C), as measured by the number of PFUs following incubation at the indicated temperatures and times. All phages were grown by complementation at 37 °C, as described in the text.

The gel pattern of C516S (Fig. 3, bottom) is similar to wt (Fig. 3, top), indicating a native-like distribution between procapsids and mature virions. Yet C516S represents a mutation that greatly accelerates portal assembly *in vitro* (Fig. 2) and generates virions of severely compromised infectivity. Hyper-assembly of the C516S portal evidently has no significant impact on either portal incorporation into procapsids or competency to package DNA. We speculate that the *in vivo* phenotype of C516S arises from a defective post-packaging event. Plausible defects are improper attachment of one or more proteins required for a fully functional tail apparatus (gp4, gp10, gp26 and/or gp9), unproductive release of DNA due to non-native interactions of the mutant portal with ejection proteins (gp7, gp16 and/or gp20) or failure of the C516S portal to achieve the conformation competent for DNA release from the capsid.

Thermostabilities of capsid-incorporated portal variants

The results of complementation assays of wt and mutant portals at different growth temperatures (28, 37, 42 and 45 °C) are compared in Table 1. *In vivo* activities of wt, C153S, C173S and C283S are essentially unchanged between 28 and 42 °C, then fall precipitously at 45 °C. On the other hand, the *in vivo* activity of C516S falls consistently between 37 and 45 °C. We infer from these results that the *in vivo* folding/assembly pathway of the C516S mutant is uniquely temperature-sensitive between 37 and 42 °C. Evidently, the relatively weak and temperature-independent S–H···X hydrogen bonding interaction of Cys 516 in the wt structure is not sustained by O–H···X interaction of Ser 516 in the mutant.

The P22 variants produced at 37 °C via the complementations described above were also incubated at 4, 45 and 55 °C to assess *in vitro* thermostabilities of the capsid-incorporated portals. The number of viable phage remaining after incubation periods of 5 and 15 h was determined by titering (Table 2). Again, we find that only C516S exhibits a significant compromise of activity with temperature, i.e. greatly diminished stability at the highest temperature tested (55 °C).

These results provide further evidence of the importance of the Cys 516 side chain for portal assembly and function.

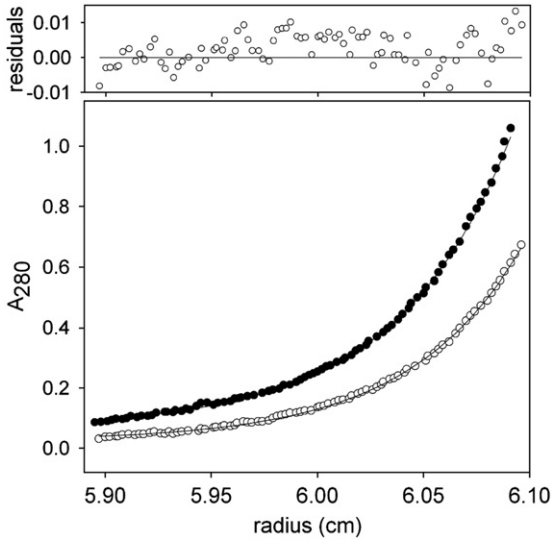

Fig. 5. Sedimentation equilibrium analysis of the wt portal dodecamer, obtained from protein solutions of 0.3 mg/mL (open circles) and 0.6 mg/mL (filled circles) concentrations spinning at 4000 RPM for 24 h. Data points were globally fitted to a single ideal solute model and the fit is shown as a continuous line through the data points. The residuals for the 0.3 mg/mL solution are shown at the top. As judged from the random distribution of residuals, the single ideal solute model produces a reasonably good fit to the experimental data.

Portal morphology

The ability of each gp1 mutant to form a portal ring assembly *in vitro* was assessed by electron microscopy. Fig. 4 compares negative stain images of *in vitro*-assembled wt and mutant portals. At this resolution, wt and mutants are indistinguishable from one another and from selected images published previously (Rodriguez-Casado and Thomas, 2003). Although earlier attempts to visualize C173S and C283S portals were not successful, owing to apparent disassembly of the rings in the low salt buffer previously employed (Rodriguez-Casado and Thomas, 2003), they are shown here to exhibit the same size

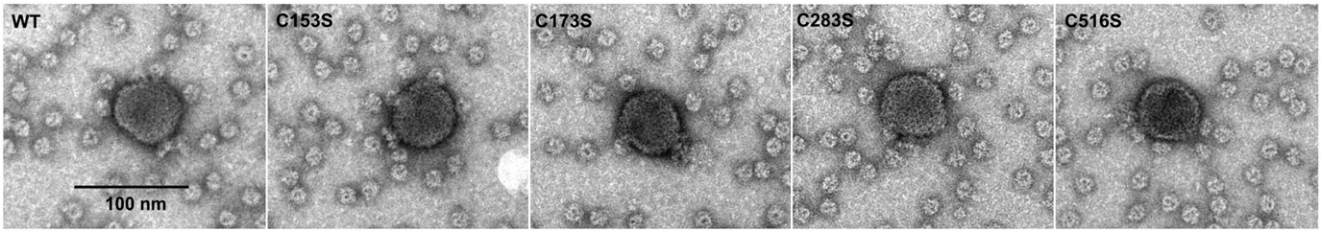

Fig. 4. Negative-stain electron micrographs (60,000×) of wild-type and mutant portals. Portal solutions (0.05 μg/μL in buffer A) containing P22 phage (~10^{11}/mL) as a size marker were deposited on copper grids, fixed with 1.0% formaldehyde and stained with 2% uranyl acetate.

Table 3
Molecular weights of wt and Cys→Ser mutant portal rings determined by sedimentation equilibrium analytical ultracentrifugation [a]

Portal	Molecular weight and standard deviation (kDa)
wt	1014±16
C153S	1005±20
C173S	1010±17
C283S	1011±14
C516S	1013±19

[a] Each molecular weight is the average of six independent determinations.

and shape as wt and other mutants. Apparently, the higher salt medium of buffer A stabilizes all of these portal variants.

Shape-independent determination of the molecular weight of each portal assembly shown in Fig. 4 was carried out by sedimentation equilibrium (SE) analysis. Representative data (A_{280} vs. radius) collected from wt portal solutions of 0.3 mg/mL and 0.6 mg/mL are shown in Fig. 5. The calculated molecular weights and standard deviations for six independent runs on each portal variant are listed in Table 3. These results indicate essentially identical molecular masses for monodisperse wt and mutant portals within the limits of experimental error. The mean molecular mass (1.011±0.005 MDa) is compatible with a 94% or greater dodecamer population. The experimental result is also consistent with the calculated molecular mass of a His_6-tagged dodecamer (1.0057 MDa).

Recently, Poliakov and coworkers have reported experimental conditions under which the P22 portal co-populates both dodecameric and undecameric states (Poliakov et al., 2007). Our measurements do not preclude the presence of a minor component of portal 11-mers, but suggest that at the experimental conditions employed here the 12-mer ring predominates.

Cysteine Raman signatures of portal variants

In a previously published analysis of the cysteine Raman signatures of wt and mutant portal rings it was concluded that mutation of one Cys site affected the local environments of other Cys sites (Rodriguez-Casado and Thomas, 2003). We have now determined that this unexpected result was due to inhomogeneities in the specific samples examined, namely the simultaneous presence of both monomers and oligomers in the C153S, C173S and C283S preparations subjected to Raman analysis. The coexistence of monomer and oligomer in each case was due to partial dissociation of the latter at the relatively low salt concentration employed (~100 mM NaCl). Here, we show the Raman results for purified homogeneous preparations of oligomeric portals stabilized in the ring form by elevation of the salt concentration (~400 mM NaCl) (Fig. 6). Oligomer stability in each case was confirmed by HPSEC analyses both before and after the Raman data collections.

The cysteine Raman spectra (2520–2620 cm^{-1}) of the portal variants are compared in Fig. 6A and the Raman signature of each cysteine site obtained by spectral subtraction is shown in Fig. 6B. Each signature reveals two S–H markers. These occur at 2565 and 2587 cm^{-1} and are diagnostic of moderately strong

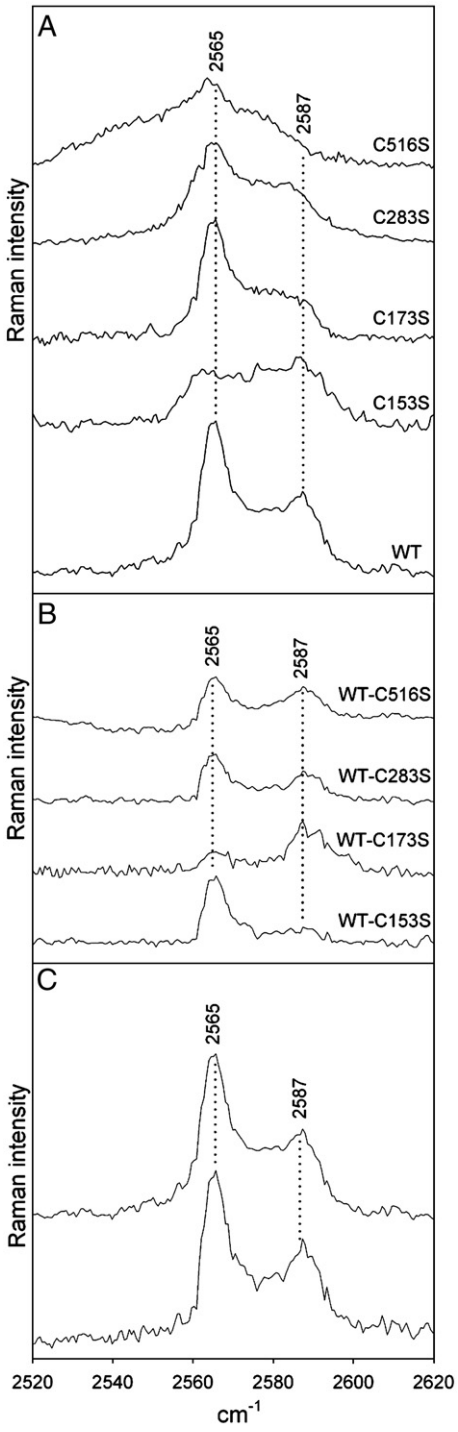

Fig. 6. (A) Raman spectra of wt and Cys→Ser mutant portal dodecamers in the region of cysteine SH stretching vibrations (2520–2620 cm^{-1}). Spectra were excited at 532 nm from 50 μg/μL solutions maintained at 4 °C. Further details of data collection are given in the text. (B) The Raman SH signature specific to each cysteine of the wt dodecamer, obtained by subtracting the appropriate mutant spectrum from the wt spectrum. (C) The upper trace shows the experimentally observed Raman spectrum of the wt portal dodecamer (from panel A) and the lower trace shows the spectrum computed by summing the four mutant spectra (from panel B). The close correspondence between the observed and computed spectra is consistent with the absence of coupling between the hydrogen bonding states of individual cysteines in the portal dodecamer.

Table 4
Sulfhydryl Raman markers and S–H···X hydrogen bond strengths of portal cysteines[a]

Cysteine residue	Raman marker (relative intensity)	Hydrogen bond strength
C153	2565 (80%)	Moderate
	2587 (20%)	Very weak
C173	2565 (24%)	Moderate
	2587 (76%)	Very weak
C283	2565 (60%)	Moderate
	2587 (40%)	Very weak
C516	2565 (50%)	Moderate
	2587 (50%)	Very weak

[a] Data are for dodecameric portal rings in 400 mM NaCl solutions. Each cysteine gives rise to two distinct Raman markers at the indicated wavenumber values (cm^{-1} units). In each case the relative intensity distribution (%) and diagnostic hydrogen bonding states are indicated (Li and Thomas, 1991).

and relatively weak S–H···X interactions, respectively. Included in the latter category are cysteines for which the SH group is exposed to solvent H_2O (Li and Thomas, 1991). The results demonstrate that each SH side chain of the wt portal protein participates in two types of hydrogen bonding interactions in the dodecamer, and that the population distribution is specific to the cysteine site. The population distributions, estimated on the basis of integrated band intensities (Li and Thomas, 1991; Raso et al., 2001), are listed in Table 4. The occurrence of multiple S–H···X states for a single cysteinyl side chain in a monodisperse protein assembly is not unprecedented and has been reported for cysteines of the native P22 tailspike trimer (Raso et al., 2001). The rank order of increasing average hydrogen bond strength in the wt portal is C173 < C516 < C283 < C153.

Fig. 6C compares the experimentally measured cysteine Raman spectrum of wt portal with that generated by summing the contributions from all individual cysteines (Fig. 6B). The excellent agreement between the experimental spectrum and the summation shows that the hydrogen bonding properties of all cysteine sites are mutually independent, as long as the integrity of each monodisperse portal is maintained (achieved here by stabilization in high salt buffer, 400 mM NaCl).

Discussion and conclusions

The portal of P22 is involved in key events of virion assembly and function, including the formation of a properly dimensioned procapsid shell and the translocation of the dsDNA genome into and out of the viral capsid during packaging and ejection, respectively. These and related functions require a stable dodecameric ring (Lander et al., 2006). In the present work we have: (*i*) applied HPSEC methods to recombinant wt and Cys → Ser mutant portals to assess the roles of subunit cysteines in dodecamer formation *in vitro*; (*ii*) used complementation assays on *1*$^{-}$ *amber* mutant P22-infected *Salmonella* cells to quantify the biological activity of wt and mutant portal dodecamers *in vivo*; (iii) used sucrose gradient separation and SDS–PAGE to characterize the composition of the cell lysate obtained from each complementation assay; (*iv*) monitored sedimentation equilibrium profiles to demonstrate that all cysteine variants of the portal form oligomeric rings of the same molecular mass (~1.006 MDa, implying a dodecamer in each case); and (*v*) re-examined Raman spectra of the wt and mutant portals to characterize local structural environments of the subunit cysteines. We have found that the dodecamer of each variant, once formed, is highly stable in 400 mM NaCl solution and is readily visualized by negative stain EM as a ring of ~20 nm outer diameter (Fig. 4). We have also found that the C283S and C516S mutants are seriously defective vis-à-vis the wt portal with regard to both *in vitro* assembly kinetics and *in vivo* activity. Conversely, the C153S and C173S mutants are similar to wt in both kinetics of dodecamer formation and biological activity. We conclude that *in vitro* assembly defects and *in vivo* activity defects of Cys → Ser portal mutants are closely correlated.

The Cys → Ser mutation at 283 generates two distinguishable functional defects vis-à-vis wt, namely retarded assembly kinetics *in vitro* and seriously reduced virion activity *in vivo*. The activity defect likely relates to portal incorporation during procapsid assembly. The stability of the C283S dodecamer is also somewhat compromised in low salt solution (Rodriguez-Casado and Thomas, 2003), which suggests a surface location that is impacted by the different hydrogen-bonding capabilities of $S^{\gamma}H$ and $O^{\gamma}H$. Interestingly, a comparative analysis of the phage P22 and φ29 portal subunit sequences (Rodriguez-Casado et al., 2001; Simpson et al., 2000) suggests that residue 283 is within a segment of the polypeptide chain that participates in intersubunit interactions. Accordingly, the present results suggest that Cys 283, by virtue of its moderate and very weak S^{γ}–H···X hydrogen bonding properties, plays a key role in subunit–subunit interactions leading to dodecamer formation and stabilization.

The Cys → Ser mutation at 516 impairs at least three functional characteristics of the P22 portal: (*i*) abnormally rapid dodecamerization kinetics *in vitro*, (*ii*) the most severely compromised *in vivo* activity of all mutants investigated (less than 20% of wt at 37 °C) and (*iii*) diminished thermal stability relative to wt when incorporated into the mature virion. Accordingly, for C516S as for C283S, we observe both *in vivo* and *in vitro* defects. The two variants are distinguished by the fact that while the *in vivo* defect of C283S is expressed at the stage of procapsid assembly, that of C516S is exhibited subsequent to DNA packaging. On the basis of the hyper-assembly rate of C516S, we speculate that proper control of dodecamerization kinetics requires participation of the Cys 516 side chain, possibly through S^{γ}–H···X hydrogen bonding (which is demonstrably weaker in the dodecamer than in the monomer). Introduction of the more robust O^{γ}–H···X hydrogen bonding potential of Ser 516 presumably compromises the essential rate-controlling role of Cys 516. Although incorporation into the procapsid and packaging of DNA are both enabled *in vivo* by the C516S portal, the majority of particles thus formed are defective at a subsequent stage of the P22 life cycle. Finally, because the C516S mutation thermally destabilizes the population of mature virions into which it has been incorporated (Table 2), we also regard Ser 516 substitution as detrimental to thermostabilization of the mature

virion. Evidently, Cys 516 is an important contributor to virion stability.

In summary, we interpret the present results as evidence that the adverse effects of the C283S and C516S mutations are due primarily to localized structural perturbations within the portal subunit rather than to global conformational changes or domain rearrangements. These localized perturbations significantly impact quaternary interactions (dodecamer assembly), but do not appreciably perturb overall subunit secondary structure (Rodriguez-Casado and Thomas, 2003). Consistent with this interpretation are the data of Fig. 6C, which show that a point mutation (Cys→Ser) at any one of the four cysteine sites does not compromise the hydrogen bonding states of the remaining three non-mutated sites. The fact that the mutation of one portal cysteine does not alter interactions of others is also in accord with findings reported previously for the P22 tailspike protein (Raso et al., 2001). Interestingly, the defects of the portal mutations studied here are manifested with the same order of impact *in vitro* (dodecamer assembly kinetics) and *in vivo* (compromised complementation), namely, C516S > C283S > C173S ≈ C153S/wt. We conclude that Cys 283 and Cys 516 participate in specific and distinct assembly-related functions that are crucial to the P22 life cycle.

Materials and methods

Expression and purification of wt and mutant (Cys→Ser) portal proteins

P22 gene *1*, which was modified to express a Leu-Glu linker and C-terminal His_6 tag, was ligated into a pET-21b plasmid and transformed into *Escherichia coli* BL21(DE3) cells (gift of Prof. Peter E. Prevelige, Jr., University of Alabama, Birmingham) (Moore and Prevelige, 2001). The product of this expression system is referred to as the wild-type (wt) protein. The expression systems for all mutants (C153S, C173S, C283S and C516S) were developed in our laboratory from the wt plasmid (Rodriguez-Casado and Thomas, 2003). The wt and mutant portal proteins were expressed and purified using Ni-affinity and anion exchange chromatographies, as described (Moore and Prevelige, 2001; Rodriguez-Casado et al., 2001; Rodriguez-Casado and Thomas, 2003). The protein eluted from the Ni column (HiTrap Chelating HP, Amersham Biosciences, Piscataway, NJ) was prepared in a buffer solution of 100 mM NaCl, 10 mM EDTA, 20 mM β-mercaptoethanol, 20 mM Tris, pH 7.9, and applied to the exchange column (HiTrap Q, Amersham Biosciences). Elution in a NaCl gradient allowed separation of the monodisperse monomer from oligomers of various sizes. The homogeneity of the monomer was verified by high performance size exclusion chromatography (HPSEC) using two SEC columns in series (model TSK6000 PWxl, TosoHaas, Montgomeryville, PA and model 330SW, Waters, Milford, MA, respectively) coupled to an AKTA protein purification system (Amersham Biosciences). Monomers and oligomers were also distinguished by dynamic light scattering measurements (data not shown). As demonstrated previously (Moore and Prevelige, 2001), the use of tandemly arranged columns resulted in complete separation of the portal monomer. On the basis of a gp1 molar extinction coefficient of 99,740 M^{-1} cm^{-1} at 280 nm, each 250-mL culture typically produced ~15 mg (wt, C283S) or ~5 mg (C153S, C173S, C516S) of the portal protein.

The portal monomers were brought to a concentration of ~0.5 mg/mL (6 μM) in 440 mM NaCl, 20 mM Tris, pH 7.5 (buffer A), and stored at −80 °C. At these conditions, all of the mutant monomers exhibited robust stability and demonstrated efficient oligomerization reactions analogous to the wt monomer. The apparent resistance to oligomer formation suggested previously for C173S and C283S based on EM data (Rodriguez-Casado and Thomas, 2003) was not encountered in the present study and can be attributed to the higher concentration of NaCl (440 vs. 100 mM) and the elimination of EDTA from the storage buffer.

Portal rings were assembled *in vitro* by elevating the monomer concentration 100-fold (~50 mg/mL, 600 μM) at 4 °C, incubating for 24 h at 22 °C, diluting the solution 50-fold and equilibrating for 6 h on ice. Portal protein was concentrated using a 50,000 MWCO Centricon concentrator (Amicon, Danvers, MA). The product was applied to a HiTrap Q column and eluted with a gradient (NaCl, 100–660 mM) to separate homogeneous dodecamers, which elute at ~650 mM NaCl (Cingolani et al., 2002) from residual monomers and heterogeneous oligomers, which elute at ~400 and ~500 mM NaCl, respectively. The homogeneity of each preparation was verified by analytical HPSEC (Moore and Prevelige, 2001; Rodriguez-Casado and Thomas, 2003). Portal dodecamers were diluted in buffer A and stored at −80 °C for subsequent use.

Electron microscopy of wt and mutant portals

For EM the *in vitro* assembled portals at 0.05 mg/mL in buffer A were mixed with ~10^{11} P22 phage/mL, the latter serving as a size standard. Solutions were applied to a carbon-coated Formvar layer supported on a copper grid. Specimens were blotted to remove excess material, fixed for 1 min with 1.0% formaldehyde and stained for 20 s with 2% uranyl acetate solution. Micrographs of the stained samples were obtained on a model 1200EX Mark II electron microscope (JEOL USA, Inc., Peabody, MA) and recorded on Kodak SO163 film at 60,000× magnification using an objective lens defocus of ~1.0 μm. All of the portal oligomers were stable in 440 mM NaCl for several days, as judged by HPSEC and EM.

Sedimentation equilibrium analyses of wt and mutant portals

Portal ring size was established by sedimentation equilibrium analyses of solutions at two concentrations, 0.3 mg/mL (A_{280}=0.35) and 0.6 mg/mL (A_{280}=0.70), using a model XL-A analytical ultracentrifuge (Beckman, Fullerton, CA). Each solution was loaded into three sample channels of a six-channel centerpiece (12-mm optical path) and analyzed for 24 h at 4000 rpm and 10 °C. The radial distribution was determined by consecutive A_{280} measurements at 0.001-cm intervals. The

absorbance profiles were fitted globally to a single ideal solute model using Beckman XL-A software (AutoR1) and assuming a partial specific volume of 0.7288 cm^3/g, as determined by the SedNTerp program (University of New Hampshire, Durham, NH). The results were plotted using Origin 6.0 software (Microcal, Northampton, MA).

In vitro assembly rates of wt and mutant portals

HPSEC was employed to compare time-dependent changes in the oligomerization states of wt and mutant portals. As noted above, two tandemly arranged columns were used for optimal separation of monomeric and dodecameric forms. Typically, a stock solution of portal monomer was concentrated to 50 μg/μL and incubated for 40–80 h on ice (4 °C). The low temperature was employed to decelerate the dodecamerization reaction so the rate of gp1 assembly could be more precisely evaluated. Aliquots were removed periodically and diluted to 0.25 μg/μL. A 10-μL aliquot of the diluted protein solution was injected into the HPSEC system and peaks were monitored at 280 nm. The time-dependent distribution of protein between monomeric and dodecameric states was determined from the corresponding peak areas.

In vivo activity and in vitro thermostability of wt and mutant portals

To evaluate the biological activity of each portal variant (wt, C153S, C173S, C283S and C516S), we carried out complementation assays using a *1⁻ amber* mutant P22 phage to infect *Salmonella* cells harboring the corresponding gp1 expressing plasmid. The five *Salmonella*-compatible plasmids and the appropriate P22 phage (*1⁻13⁻ amber* mutant) were gifts from Prof. Peter E. Prevelige (University of Alabama, Birmingham) (Moore and Prevelige, 2002a). (The *13⁻* mutation enhances accumulation of progeny phage by preventing cell lysis.) Each portal-expressing plasmid was transformed by electroporation into competent *Salmonella* cells. Each of the five cell lines was infected with the *1⁻13⁻ amber* mutant (MOI=1), while simultaneously being induced with 0.46 mM IPTG to express gp1. (This IPTG concentration allows optimal production of phage in the complementation assays (Moore and Prevelige, 2002b).) The culture was incubated for 3 h at 37 °C. A 100 μL aliquot was removed from the culture at time points of 0 and 10 min to establish the quality of the infection and at 3 h to test for complementation. The cells in each aliquot were lysed, and the supernatant was titered on a *Salmonella* suppressor. Biological activity was quantified by the number of infectious particles produced during each assay. As a negative control, the complementation assay was also performed using *Salmonella* cells that did not contain the gp1 expressing plasmid. In the absence of the plasmid, no P22 phage were produced after infection with the *1⁻13⁻ amber* mutant. Temperature sensitivity of portal biological activity was assessed by conducting similar complementation assays at 28, 42 and 45 °C.

To further characterize the *in vivo* activity of each portal variant, cell lysates from the complementation assays described above were assessed by sucrose gradient separation and SDS–PAGE. Each cell lysate was applied to a linear sucrose gradient (5–45%) to separate by weight the soluble components. The gradients were spun at 35,000 rpm in an SW41 rotor (Beckman, Fullerton, CA) and an L8-80M ultracentrifuge (Beckman, Fullerton, CA). The resulting gradients were fractionated (twelve 1-ml fractions) and an aliquot of each fraction was evaluated with SDS–PAGE and Coomassie blue staining to detect the relative amounts of portal, scaffolding and capsid proteins.

In vitro thermostabilities of wt and mutant portals – once incorporated into mature phage particles that had been assembled at 37 °C – were assessed by titering the phage following incubations at selected temperatures in the range 4–55 °C.

Raman spectroscopy of wt and mutant portals

Stock solutions of dodecameric portal protein (1 μg/μL in buffer A) were concentrated to 50 μg/μL in a Centricon-50 device (Amicon, Danvers, MA). Typically, a 5-μL aliquot of the concentrated solution was transferred to a thin-walled 1-mm glass capillary (Kimax no. 34502). Raman spectra were excited at 532 nm (Verdi 5W laser, Coherent Inc., Santa Clara, CA) and collected using a single-grating spectrograph (model Spex 500M, ISA, Edison, NJ) equipped with a holographic notch filter, holographic grating and a back-thinned, liquid nitrogen-cooled charge-coupled device detector (Spectrum One, ISA, Edison, NJ). Further details of the Raman instrumentation have been described elsewhere (Movileanu et al., 1999; Rodriguez-Casado and Thomas, 2003). Sample cells were sealed and thermostatted (4 °C) for data collections. The Raman spectra shown below (2520–2620 cm^{-1}) represent averages of 50 exposures of 240 s each, for a total exposure time of ~3 h per protocol. All results were duplicated on independently prepared samples. Laser illumination and related sample handling resulted in no time-dependent spectral changes, consistent with earlier findings (Rodriguez-Casado et al., 2001; Rodriguez-Casado and Thomas, 2003).

Acknowledgment

Supported by NIH Grant GM50776.

References

Bazinet, C., King, J., 1988. Initiation of P22 procapsid assembly in vivo. J. Mol. Biol. 202, 77–86.

Bazinet, C., Benbasat, J., King, J., Carazo, J.M., Carrascosa, J.L., 1988. Purification and organization of the gene *1* portal protein required for phage P22 DNA packaging. Biochemistry 27, 1849–1856.

Botstein, D., Waddell, C.H., King, J., 1973. Mechanism of head assembly and DNA encapsulation in Salmonella phage P22: I. Genes, proteins, structures and DNA maturation. J. Mol. Biol. 80, 669–695.

Casjens, S., Weigele, P., 2005. DNA packaging by bacteriophage P22. In: Catalano, C.E. (Ed.), Viral Genome Packaging Machines: Genetics, Structure, and Mechanism. Landes Bioscience/Eurekah.com, Georgetown, TX and Kluwer Academic/Plenum Publishers, New York, pp. 80–88.

Casjens, S., Wyckoff, E., Hayden, M., Sampson, L., Eppler, K., Randall, S., Moreno, E.T., Serwer, P., 1992. Bacteriophage P22 portal protein is part of

the gauge that regulates packing density of intravirion DNA. J. Mol. Biol. 224, 1055–1074.

Cingolani, G., Moore, S.D., Prevelige Jr., P.E., Johnson, J.E., 2002. Preliminary crystallographic analysis of the bacteriophage P22 portal protein. J. Struct. Biol. 139, 46–54.

Eppler, K., Wyckoff, E., Goates, J., Parr, R., Casjens, S., 1991. Nucleotide sequence of the bacteriophage P22 genes required for DNA packaging. Virology 183, 519–538.

Fane, B.A., Prevelige Jr., P.E., 2003. Mechanism of scaffolding-assisted viral assembly. Adv. Protein Chem. 64, 259–299.

Fuller, M.T., King, J., 1980. Regulation of coat protein polymerization by the scaffolding protein of bacteriophage P22. Biophys. J. 32, 381–401.

Greene, B., King, J., 1996. Scaffolding mutants identifying domains required for P22 procapsid assembly and maturation. Virology 225, 82–96.

King, J., Lenk, E.V., Botstein, D., 1973. Mechanism of head assembly and DNA encapsulation in Salmonella phage P22: II. Morphogenetic pathway. J. Mol. Biol. 80, 697–731.

King, J., Botstein, D., Casjens, S., Earnshaw, W., Harrison, S., Lenk, E., 1976. Structure and assembly of the capsid of bacteriophage P22. Philos. Trans. R. Soc. Lond., B Biol. Sci. 276, 37–49.

Lander, G.C., Tang, L., Casjens, S.R., Gilcrease, E.B., Prevelige Jr., P.E., Poliakov, A., Potter, C.S., Carragher, B., Johnson, J.E., 2006. The structure of an infectious P22 virion shows the signal for headful DNA packaging. Science 312, 1791–1795.

Li, H., Thomas Jr., G.J., 1991. Cysteine conformation and sulfhydryl interactions in proteins and viruses: I. Correlation of the Raman S–H band with hydrogen bonding and intramolecular geometry in model compounds. J. Am. Chem. Soc. 113, 456–462.

Moore, S.D., Prevelige Jr., P.E., 2001. Structural transformations accompanying the assembly of bacteriophage P22 portal protein rings in vitro. J. Biol. Chem. 276, 6779–6788.

Moore, S.D., Prevelige Jr., P.E., 2002a. A P22 scaffold protein mutation increases the robustness of head assembly in the presence of excess portal protein. J. Virol. 76, 10245–10255.

Moore, S.D., Prevelige Jr., P.E., 2002b. Bacteriophage P22 portal vertex formation in vivo. J. Mol. Biol. 315, 975–994.

Movileanu, L., Benevides, J.M., Thomas, G.J., 1999. Temperature dependence of the Raman spectrum of DNA: I. Raman signatures of premelting and melting transitions of poly(dA–dT)·poly(dA–dT). J. Raman Spectrosc. 30, 637–649.

Newcomb, W.W., Thomsen, D.R., Homa, F.L., Brown, J.C., 2003. Assembly of the herpes simplex virus capsid: identification of soluble scaffold–portal complexes and their role in formation of portal-containing capsids. J. Virol. 77, 9862–9871.

Poliakov, A., Duijn, E.V., Lander, G., Fu, C.Y., Johnson, J.E., Prevelige Jr., P.E., Heck, A.J., 2007. Macromolecular mass spectrometry and electron microscopy as complementary tools for investigation of the heterogeneity of bacteriophage portal assemblies. J. Struct. Biol. 157, 371–383.

Prevelige Jr., P.E., King, J., 1993. Assembly of bacteriophage P22: a model for ds-DNA virus assembly. Prog. Med. Virol. 40, 206–221.

Raso, S.W., Clark, P.L., Haase-Pettingell, C., King, J., Thomas Jr., G.J., 2001. Distinct cysteine sulfhydryl environments detected by analysis of Raman S–H markers of Cys→Ser mutant proteins. J. Mol. Biol. 307, 899–911.

Rodriguez-Casado, A., Thomas Jr., G.J., 2003. Structural roles of subunit cysteines in the folding and assembly of the DNA packaging machine (portal) of bacteriophage P22. Biochemistry 42, 3437–3445.

Rodriguez-Casado, A., Moore, S.D., Prevelige Jr., P.E., Thomas Jr., G.J., 2001. Structure of bacteriophage P22 portal protein in relation to assembly: investigation by Raman spectroscopy. Biochemistry 40, 13583–13591.

Simpson, A.A., Tao, Y., Leiman, P.G., Badasso, M.O., He, Y., Jardine, P.J., Olson, N.H., Morais, M.C., Grimes, S., Anderson, D.L., Baker, T.S., Rossmann, M.G., 2000. Structure of the bacteriophage φ29 DNA packaging motor. Nature 408, 745–750.

Strauss, H., King, J., 1984. Steps in the stabilization of newly packaged DNA during phage P22 morphogenesis. J. Mol. Biol. 172, 523–543.

Tang, L., Marion, W.R., Cingolani, G., Prevelige Jr., P.E., Johnson, J.E., 2005. Three-dimensional structure of the bacteriophage P22 tail machine. EMBO J. 24, 2087–2095.

Trus, B.L., Cheng, N., Newcomb, W.W., Homa, F.L., Brown, J.C., Steven, A.C., 2004. Structure and polymorphism of the UL6 portal protein of herpes simplex virus type 1. J. Virol. 78, 12668–12671.

Weigele, P.R., Sampson, L., Winn-Stapley, D., Casjens, S.R., 2005. Molecular genetics of bacteriophage P22 scaffolding protein's functional domains. J. Mol. Biol. 348, 831–844.